CROSS SECTIONS, PROBABILITIES, MULTIPLICITIES AND SPECTRA OF SECONDARIES IN HIGH ENERGY HEAVY ION INTERACTIONS

J.Dias de Deus and Yu.M.Shabelski*

CENTRA, Instituto Superior Tecnico, 1049-001 Lisboa, Portugal

Abstract

We present a short review of theoretical results (mainly for experimentalists) published in many different papers. The formulae are presented for the different integrated cross sections, the number of interacting nucleons, multiplicities of secondaries, the dispersions of multiplicity distributions. Two possible tests for the search of Quark-Gluon Plasma formation are discussed. CERN SPS data for production of secondaris in central Pb+Pb collisions are compared with Quark-Gluon String Model predictions.

Permanent address:
Petersburg Nuclear Physics Institute,
Gatchina, St.Petersburg 188350 Russia

1

1 Introduction

At present time, different Monte Carlo codes are used, as a rule, for the analyses of existing heavy ion experiments and for planning the future ones. However, sometimes it is not clear enough, what physics was used in some Monte Carlo code, which processes were accounted for, and so on. In the present paper we give a review of the simplest theoretical predictions which can be used for different estimates, not involving complicated calculations.

Formally we consider the high energy nucleus-nucleus collision as a superposition of the independent nucleon-nucleon interactions. However, really the main part of the discussed results is based practically only on geometry, and does not depend on the model of interaction.

2 Cross sections

Let us consider the collision of nucleus A with nucleus B, assuming that they are not very light. The simplest expression for the total inelastic σ_{AB}^{in}, or secondary production cross section σ_{AB}^{prod} comes from geometry:

$$\sigma_{AB}^{in} \approx \sigma_{AB}^{prod} = \pi(R_A + R_B)^2 \ . \tag{1}$$

The difference between σ_{AB}^{in} and σ_{AB}^{prod}, which corresponds to all processes of disintegration or exitation of one or both nuclei without secondary production, is negligibly small at high energies and heavy incident nuclei. In the case of heavy ion collisions the total elastic cross section is only slightly smaller than σ_{AB}^{in} [1], $\sigma_{AB}^{el} \approx \sigma_{AB}^{in}$, so

$$\sigma_{AB}^{tot} = \sigma_{AB}^{el} + \sigma_{AB}^{in} = 2\pi(R_A + R_B)^2 \ . \tag{2}$$

More accurate is Bradt-Peters expression [2]

$$\sigma_{AB}^{in} = \pi R_0^2 (A^{1/3} + B^{1/3} - c)^2 \ , \tag{3}$$

which accounts for the possibility of very peripheral collisions without inelastic interactions. The values of parameters R_0 and c are slightly different for light and heavy nuclei [1]. The comparison of this expression with the experimental data was presented in [3].

More detailed results for different cross sections of heavy ion interactions can be obtained with the help of multiple scattering (Glauber) theory, see [4] for details. This theory can be used at all energies starting from several hundred MeV per nucleon. At high energies (say, more than 10 GeV per nucleon) in principle the inelastic screening [5, 6] should be accounted for,

however in the case of heavy ion cross sections these effects are numerically very small.

The amplitude of $A - B$ elastic scattering with momentum transfer q can be written in the frame where B-nucleus is a fixed target as

$$F_{AB}^{el}(q) = \frac{ik}{2\pi} \int d^2 b e^{iqb} [1 - S_{AB}(b)] , \qquad (4)$$

where k is the incident momentum of one nucleon in A-nucleus, b - impact parameter, and

$$S_{AB}(b) = \langle A| \langle B| \prod_{\substack{i\in A \\ j\in B}} [1 - \Gamma_{NN}(b + u_i - s_j)] \, |B\rangle |A\rangle , \qquad (5)$$

$$\Gamma_{NN}(b + u_i - s_j)] = \frac{1}{2\pi ik} \int d^2 q e^{-iq(b+u_i-s_j)} f_{NN}(q) , \qquad (6)$$

where u_i and s_i are the transverse coordinates of nucleons. Contrary to the case of hadron-nucleus interaction, we can not integrate Eq. (5) analitically even after standard assumption that nuclear density is a product of one-nucleon densities.

To make the problem manageable, one can pick up a certain fraction only of various contributions in the expansion of the product in Eq. (5), distinguished by large combinatorial factors. The leading graphs correspond to the so-called optical approximation [7], which sums up the contributions with scattering not more than once for each nucleon, i.e. takes into account the products of amplitudes Γ_{NN} in Eq.(5) with all indices i, j being different. It corresponds to the summation of diagrams shown in Fig. 1 and it contain the largest combinatorial factor $A(A-1)...(A-n+1)B(B-1)...(B-n+1)$ in the case of n-fold interaction. In all another series the combinatorial factors are significantly smaller, however these series have different signs, so due to the large cancelation some of them can give significant contribution to the final expression. To avoid crowding of lines we have only shown in Fig. 1 the nucleon participants from the nucleus A (upper dots) and B (lower dots) with the links standing for interacting amplitudes, and we do not plot the nucleon-spectators.

In the language of Eq. (5) the optical approximation can be reproduced, making the averaging $\langle A|...|A\rangle$ and $\langle B|...|B\rangle$ inside the product $\prod_{i,j}$ in Eq.(5) instead of averaging the product as a whole:

$$S_{AB}^{opt}(b) = \prod_{i,j} \langle A| \langle B| [1 - \Gamma_{NN}(b + u_i - s_j)] \, |B\rangle |A\rangle , \qquad (7)$$

Using the standard assumptions of the multiple scattering theory one obtains

$$S_{AB}^{opt}(b) = \left[1 - \frac{1}{A} T_{opt}(b)\right]^A \approx exp[-T_{opt}(b)] \qquad (8)$$

3

with

$$T_{opt}(b) = \sigma/2 \int d^2b_1 T_A(b_1 - b) T_B(b_1) \tag{9}$$

and

$$T_A(b) = A \int_{-\infty}^{\infty} dz \rho(b = \sqrt{r^2 - z^2}, z) \tag{10}$$

where $\rho(r)$ is the one-particle nuclear density, $\int \rho(r) d^3 r = 1$.

In the Reggeon language the optical approximation corresponds to the accounting only one pole (nuclear ground state) in the both M_A^2 and M_B^2 complex planes instead of all intermediate states, see [4].

However, numerical calculations [8] (see also [9] for the case of light nuclei collision) demonstrate that the optical approximation is not accurate enough even for the total cross sections. The difference with the data amounts $\sim$ 10-15% for σ_{AB}^{tot} and is much larger for differential cross sections.

The more explicit rigid target [10, 11, 12, 13] approximation can be reproduced, making the averaging only $\langle B|...|B \rangle$ inside the product in Eq. (5) :

$$S_{AB}^{r.g.}(b) = \langle A|\{\prod_{i,j} |\langle B|[1 - \Gamma_{NN}(b + u_i - s_j)] |B\rangle\}|A\rangle = [T_{r.g.}(b)]^A , \tag{11}$$

$$T_{r.g.}(b) = \frac{1}{A} \int d^2b_1 T_A(b_1 - b) exp \left[-\frac{\sigma}{2} T_B(b_1) \right] , \tag{12}$$

This approach corresponds to the diagrams of Fig. 2, where each nucleon from the nucleus A can interact several times, but all interacting nucleons from B are still different. Due to the obvious asymmetry in contributions of the two nuclei such approach can be justified theoretically in the limit $A/B \ll 1$, say for $C - Pb$, or $S - U$ collisions, however sometimes it can be used for the case of heavy ion collisions with equal atomic weights, see next Sect.

Further corrections to the elastic amplitude have been considered in Refs. [14, 15, 16, 17, 18], however these results are rather complicated for practical use.

Another possibility is the direct calculation of Eq. (5) using Monte Carlo simulation [1, 19].

Let us present now the list of several integrated cross sections. The total cross section of $A - B$ collision is given by the optical theorem

$$\sigma_{AB}^{tot} = 2 \int d^2b[1 - S_{AB}(b)] , \tag{13}$$

where the function $S_{AB}(b)$ can be taken, say, from Eq. (8) or Eq. (11). The integrated cross section of elastic $A - B$ scattering is

$$\sigma_{AB}^{el} = \int d^2b[1 - S_{AB}(b)]^2 . \tag{14}$$

The sum of cross sections of all diffractive processes without production of secondaries, i.e. the elastic and quasielastic scattering can be calculated with the help of close approximation $\sum_{A'} |A'\rangle\langle A'| = 1$ similarly to the case of hadron-nucleus scattering [20]

$$\sigma_{AB}^{scat} = \int d^2b\{1 - 2S_{AB}(b) + [I_{AB}(b)]^A\} , \qquad (15)$$

where in the optical approximation

$$I_{AB}^{opt}(b) = 1 - \frac{1}{A}R_{opt}(b) , \qquad (16)$$

$$R_{opt}(b) = \sigma^{inel} \int d^2b_1 T_A(b_1 - b)T_B(b_1) \qquad (17)$$

and σ^{inel} is the NN inelastic cross section. In the rigid target approximation

$$I_{AB}^{r.t.}(b) = \frac{1}{A} \int d^2b_1 T_A(b_1 - b)exp[-\sigma^{inel}T_B(b_1)] \qquad (18)$$

The correspondent expression for the secondary production cross section reads

$$\sigma_{AB}^{prod} = \sigma_{AB}^{tot} - \sigma_{AB}^{scat} = \int d^2b\{1 - [I_{AB}]^A\} . \qquad (19)$$

It is also possible [21] to obtain the integrated stripping cross sections of collisions among light nuclei. This can be done by considering the different intermediate states [22, 23, 9] of all Glauber diagrams for elastic AB amplitude. The resulting expressions have the simple form of a combination of several total inelastic cross sections. For example, the cross section for stripping one nucleon from nucleus A in A-B collision, $\sigma_{AB}^{(1)}$, is written as

$$\sigma_{AB}^{(1)} = A(\sigma_{AB}^{inel} - \sigma_{(A-1)B}^{inel}) , \qquad (20)$$

where the density distribution of the nucleus with atomic weight A-1 should be slightly "corrected" [21]

3 Distributions on the number of interacting nucleons

Let us consider the events with secondary hadron production in nuclei A and B minimum bias collisions. In this case the average number of inelastically interacting nucleons of a nucleus A is equal [24] to

$$< N_A >_{m.b.} = \frac{A\sigma_{NB}^{prod}}{\sigma_{AB}^{prod}} . \qquad (21)$$

If both nuclei, A and B are heavy enough, the production cross sections of nucleon-nucleus and nucleus-nucleus collisions can be written as

$$\sigma_{NB}^{prod} = \pi R_B^2 , \quad \sigma_{AB}^{prod} = \pi (R_A + R_B)^2 , \qquad (22)$$

and accounting for Eq. (1) we obtain that in the case of equal nuclei, A = B, for minimum bias (m.b.) events which are averaged over impact parameter

$$< N_A >_{m.b.} = A/4 = < N_A >_c /4 . \qquad (23)$$

So in the case of minimum bias events the average number of interacting nucleons should be four times smaller than in the case of central collisions [25], where (neglecting by small corrections which will be discussed below) $< N_A >_c \approx A$.

The average number of inelastic NN interactions in minimum bias AB collisions with any secondary production is equal [3, 13] to

$$< \nu_{AB} >_{m.b.} = AB\sigma_{NN}^{inel}/\sigma_{AB}^{prod} . \qquad (24)$$

Let us note that the optical approximation cannot be used [3] for the calculations of the averaged numbers of interacting nucleons and the distribution on this number. The rigid target approximation gives here reasonable results. In particular, for the distribution over the number of inelastically interacting nucleons N_A of A nucleus in AB interaction we have [12]

$$V(N_A) = \frac{1}{\sigma_{AB}^{prod}} \frac{A!}{(A - N_A)!N_A!} \int d^2 b [I_{AB}^{r.t.}(b)]^{A-N_A} [1 - I_{AB}^{r.t.}(b)]^{N_A} , \qquad (25)$$

The theoretical predictions for the distributions on the electrical charge of non-interacting nucleons based on Eq. (25) were compared with the data in [12] and the agreement was quite reasonable, see Fig. 3 taken from [12].

All the presented results are related to the case when only the events with secondary production are registered. In the case when the events with nuclear disintegration without secondary production are also registered, one should change σ_{NN}^{inel} by σ_{NN}^{tot} and σ_{AB}^{prod} by σ_{AB}^{inel}.

Eq. (25) is written for minimum bias events. In the case of events for some interval of impact parameter b values, the integration in Eq. (25) should be fulfilled by this interval, $b_{min} < b < b_{max}$. In particular, in the case of central collisions the integration should be performed with the condition $b \leq b_0$, and $b_0 \ll R_A$. In the case of the collisions of equal heavy ions the value of $< N_A >$ decreases with increase of the impact parameter. As even at small $b \neq 0$ some regions of colliding ions are not overlapping, only very small fraction of events, not larger than 0.5-0.7% of all minimum bias sample, can be considered as the central interactions.

In the case of asymmetrical ion collisions, say $S - U$, all nucleons of light nucleus at small impact parameters go throw the regions of relatively high nuclear matter density of heavy nucleus, so practically all these nucleons interact inelastically. For the case of $S - U$ interactions at $\sqrt{s_{NN}} = 20$ GeV all events with $b < 2 \div 3$ fm can be considered as the central ones [25].

The predictions for the distributions on the number of inelastically interacting nucleons at different impact parameters can be found in [25].

4   Multiplicities of secondaries, inclusive densities and tests for QGP formation

Let us now look at the inclusive density of the produced secondaries,

$$\rho_{AB}(x) = E \frac{d^3 \sigma^{AB}}{d^3 p} \ . \tag{26}$$

In the case of asymptotically high energies we predict[1] for $x_F \to 0$ [3]

$$\rho_{AB}(x)/\rho_{NN}(x) = < \nu_{AB} > \tag{27}$$

and for secondary multiplicities

$$< n_{AB} > / < n_{NN} > = < \nu_{AB} > \tag{28}$$

However at the realistic energies both right-hand side ratios (27) and (28) are significantly smaller than the predicted values due to the energy conservation corrections. For example, if one nucleon of the projectile nucleus interact with several nucleons of the target nucleus, the total energy of all secondaries should be equal to the initial energy, so the effective energy of every NN interaction is smaller than the initial energy. These effects are more important in the both A and B fragmentation regions.

The corrections to Eqs. (27) and (28) decrease with the growth of the initial energy. Some predictions for the multiplicity of secondaries with accounting the division of energy between several NN interactions can be found in [28].

The relations between average multiplicities and inclusive densities of secondaries produced in heavy ion collisions can be used for search of the Quark-Gluon Plasma (QGP) formation. One of them is the relation between average

---

[1]We do not account here the additional shadowing due to percolation [26] or multiple pomeron interactions [27].

multiplicity and inclusive density in the central region. In the case of NN collisions for any $z = n_{-NN}/ < n_{-NN} >)$ the ratio [2]

$$R(z) = \rho_{NN}(x)/ < \rho_{NN}(x) > |_{x \sim 0} \qquad (29)$$

is a non-trivial function of z [29]. The reason is again in energy conservation. Let us compare two events, first with $n_- = < n_- >$ and second with $n_- = 2 < n_- >$. Evidently, if the shapes of the inclusive spectra in these events will be the same, the energy of all secondaries in the second event will be two times larger than in the first one. So the shapes should be different, in the second event we will find smaller number of fast secondaries and larger number of slow ones. The experimental data [30] as well as the model calculations [29] show that the ratio $R(z) = \rho_{NN}(x)/ < \rho_{NN}(x) > |_{x \sim 0}$ is about 3.5 at $z = 2.5$.

However, in the case of heavy ion collisions with independent nucleon-nucleon interactions we can not expect any difference of Eq. (29) from the linear function, because every independent nucleon-nucleon collision gives the same contribution to $\rho_{(x)}$ as well as to multiplicity [3]. The possible violation of such linear dependence should be considered as an evidence for some collective interaction (possibly, QGP formation). The analysis of the data at energy about 4 GeV per nucleon [31] shows good agreement with linear dependence, and the similar analysis of the data at higher energies seems to be very interesting. Such analysis can be provided in some kinematical domain.

The second test for QGP formation is connected with analysis of the multiplicities of different secondaries produced in the central and minimum bias $A - B$ collisions [25]. In the case of independent nucleon-nucleon collisions the multiplicity of secondaries produced in the central region should be proportional to the number of interacting nucleons of projectile nucleus, that is four times larger than in minimum bias events, see Eq. (23). It should depends also on the average number, $< \nu_{NB} >$, of inelastic interactions of every projectile nucleon with the target nucleus. As was shown in [32], the average number of interactions in the case of central nucleon-nucleus collisions, $< \nu >_c$, is approximately 1.5 times larger than in the case of minimum bias nucleon-nucleus collisions, $< \nu >_{m.b.}$. After accounting several another

---

[2]The considering ratio is rather similar to KNO one, however instead of cross sections we use inclusive densities.

[3]The difference in heavy ion and NN interactions here is connected both with experimental conditions and with confinement. In heavy ion collisions we usually registrate only the interacting nucleons and neglect the non-interacting ones. Due to that the energy of secondaries can change from event to event. In the case of NN interaction the spectator quarks and gluons will be involved into the interaction due to confinement forces, and the energy of all secondaries is exactly equal to the initial energy.

corrections [25] one obtain

$$<n>_c \sim 4.5 <n>_{m.b.} \quad . \tag{30}$$

In the conventional approach considered here, we obtain the prediction of Eq. (30) for any sort of secondaries including pions, kaons, J/ψ, Drell-Yan pairs, direct photons, etc. Let us imagine that the QGP formation is possible (or dominate) only at comparatively small impact parameters, i.e. in the central interactions. In this case Eq. (30) can be strongly violated, say, for direct photons and, possibly, for light mass Drell-Yan pairs, due to the additional contribution to their multiplicity in the central events via the thermal mechanism. At the same time, Eq. (30) can be valid, say, for high mass Drell-Yan pairs and for pions, if the most part of them is produced at the late stage of the process, after decay of the plasma state. So the experimental confirmation of Eq. (30), say, for pions and its violation for the particles which can be emitted from the plasma state should be considered as a signal for QGP formation. Of course, the effects of final state interactions, etc. should be accounted for in such test.

5   Multiplicity distributions and dispersions

It was shown in Ref. [33] that the main contribution to the dispersion of multiplicity distribution in the case of heavy ion collisions comes from the dispersion in the number of nucleon-nucleon interactions. The last number is in strong correlation with the value of impact parameter.

For the normalized dispersion $D/<n>$, where $D^2 =<n^2> - <n>^2$ we have [33]

$$\frac{D^2}{<n>^2} = \frac{<\nu_{AB}^2> - <\nu_{AB}>^2}{<\nu_{AB}>^2} + \frac{1}{<\nu_{AB}>}\frac{d^2}{\overline{n}^2} \ , \tag{31}$$

where

$$<\nu_{AB}> = <N_A> \cdot <\nu_{NB}> \tag{32}$$

is the average number of nucleon-nucleon interactions in nucleus-nucleus collision, $\overline{n}$ and d are the average multiplicity and the dispersion in one nucleon-nucleon collision.

In the case of heavy ion collisions $<\nu_{AB}> \sim 10^2 - 10^3$, so, as a rule, the second term in the right hand side of Eq. (31) becomes negligible [33], and the first term, which is the relative dispersion in the number of nucleon-nucleon interactions, dominates. In the case of minimum bias A-B interaction the last dispersion is comparatively large due to large dispersion in the distribution on N_A (ν_{AB}). So in the case of some trigger (say, J/ψ production) without

9

fixing of the impact parameter, the multiplicity of all another secondaries can change significantly in comparison with its average value.

In the case of some narrow region of impact parameters we have the opposite situation. Dispersion in the distribution on N_A (ν_{AB}) is very small [25], especially in the case of central collisions. The dispersion in the number of inelastic interactions of one projectile nucleon with the target nucleus, ν_{NB}, should be the same or slightly smaller in comparison with the minimum bias case. So the dispersion in the multiplicity of the produced secondaries can not be large.

If fluctuations in the effective number of interactions are negligible, the second term in the right hand side of Eq. (31) should dominate and the dispersion of the produced secondaries will be suppressed by the factor $< \nu_{AB} >$ in comparison with the case of NN collisions.

In the case of small fluctuations in ν_{AB} one can see that any trigger can not change significantly the average multiplicity of secondaries in the central heavy ion collisions, even if this trigger strongly influents on the multiplicity in the nucleon-nucleon interaction.

Some numerical example of very narrow secondary multiplicity distribution in central heavy ion collisions can be found in [28].

Now let us consider some rare event C in high energy heavy ion collisions. It can be Drell-Yan heavy mass pair, J/Ψ, Υ, W or Z production. The normalized multiplicity distribution of the produced secondaries in the events associated to such rare events, $P_C(n)$, should be not the same as the distribution in the mimimum bias events, $P_{m.b.}(n)$, with $\sum Pm.b.(n) = \sum P_C(n) = 1$. The reason is quite clear. The rare events can occur independently in every NN collision, so in the case of heavy ion interactions the probability of rare event is proportional to ν_{AB}, Eq. (32). So [34]

$$P_C(n) = \frac{\nu_{AB}}{< \nu_{AB} >} P(n) \qquad (33)$$

The experimental data at high energies are in agreement with the prediction of Eq. (33). An example of such agreement is presented in Fig. 4, taken from [34]. The similar relation can be written for the distributions on the transverse energy, E_T [35, 36], etc., and they are in agreement with existing high energy data [34, 35].

6 Spectra of secondaries

As we discussed, the energy conservation effects violate asymptotical ratios (27) and (28). The possible way to account for these effects was suggested

in [28, 32]. The inclusive spectrum of secondaries produced in nucleus A - nucleus B collision can bew written as

$$\frac{1}{\sigma_{AB}^{prod}} \frac{d\sigma(AB \to hX)}{dy} = \theta(y) R_A^h(y) < N_A > \frac{1}{\sigma_{NB}^{prod}} \frac{d\sigma(NB \to hX)}{dy} + \quad (34)$$

$$+ \quad \theta(-y) R_B^h(-y) < N_B > \frac{1}{\sigma_{NA}^{prod}} \frac{d\sigma(NA \to hX)}{dy} \ ,$$

where y is the rapidity of secondary h in c.m. frame and the functions $R_{A,B}^h(y)$ account for the energy conservation effects. Here we connect the inclusive spectra of secondaries in the heavy ion collisions with the spectra in the nucleon-nucleus interactions. To calculate the last ones as well as the functions $R_{A,B}^h(y)$ we use one of the variants of the dual topological unitarization approach - the quark-gluon string model (QGSM) [37]. This model has been used successfully to describe the spectra of secondaries produced on both nucleon [37, 38, 39] and nuclear [40, 41] targets. In QGSM the high-energy interaction is determined by an exchange of one or several pomerons. One pomeron is coupled to a valence quark and diquark, and the others are coupled to sea quark-antiquark pairs. All elastic and inelastic processes are the result of a cut of different number of pomerons or a cut between pomerons [22]. The inclusive spectra of secondaries are determined by convolutions of the quark and diquark momentum distributions and the functions describing their fragmentation into hadrons. All these functions are determined by their Regge asymptotics. When one nucleon interacts with several, the average number of pomerons is increased, which tends to soften the momentum distributions of all quarks and diquarks and, consequently, the secondary hadron spectra.

The functions $R_{A,B}^h(y)$ can be taken in the form [28, 32]

$$R_A^h(y) = \frac{f^h(-y, <\nu>_{NA})}{<\nu>_{NA} f^h(-y, 1)} \ , \quad (35)$$

where $f^h(y, <\nu>)$ is the contribution from the interaction with ν nucleons to the spectrum of secondary particle h in NA collision.

The results of secondary spectra calculation in the QGSM depend on several parameters. They can be fixed from pp data. The values of parameters were changed slightly in comparison with [39], because new experimental data have appeared. The results for the x_F-spectra of secondary π^+, π^-, K^+ and K^- are presented in Fig. 5. The agreement with the data [42, 43] is quite reasonable. The description of secondary proton and antiproton spectra (agreement with the data is of the same order) one can find in [44].

The rapidity distributions of secondary π^+, π^-, K^+, K^-, p and $\bar{p}$ measured in $Pb+Pb$ central collisions at 158 GeV/c per nucleon [45] are compared with

our calculations using Eq. (34) in Fig. 6 .In the case of pions the agreement is reasonable. The differences between the calculated curves and the data are larger than 10%. In the case of secondary kaons we see that there is a problems.

The spectrum of K^- is in good agreement with the model, whereas for K^+ disagreement is about 20%. In the case of change of the model parameters one will obtain the disagreement in Figs. 5c and 5d. Even more serious is the K^+/K^- ratios. Experimentally this ratio at $y \sim 0$ is about 1.5, however in the model we can not obtain it more than 1.2. It means that the sea contribution (which leads to the same yields of K^+ and K^-) is too large in the model. It is possible, that the account for percolation/string fusion effect [26, 47, 48] as well as final state interactions [46] can solve this problem.

In the cases of p and $\bar{p}$ the agreement with the data is good enough.

7   Conclusions

We presented some simplest and model independent formulae obtained with assumption that high energy heavy ion collision can be consider as the superposition of independent nucleon-nucleon collisions. So any serious disagreement of these predictions with the data can be considered as the signal for some collective interaction, say QGP formation.

Contrary to the case of elementary particle physics the numerical results for heavy ion collisions should be obtained correspondently to the experimental conditions. For example, if only events with secondary production are registrated one should use Eqs. (21) and (24), whereas if events with nuclear disintegration and without secondary production are also registrated, the cross sections σ_{AB}^{prod}, σ_{NB}^{prod} and σ_{NN}^{inel} should be replaced by σ_{AB}^{inel}, σ_{NB}^{inel} and σ_{NN}^{tot}, respectively.

The results for rapidity spectra of secondaries are more model dependent. It is possible that the effects of inclusive density saturations are observed at CERN SppS energies, and the new RHIC data also give evidences for such effects.

Figure captions

Fig. 1. The optical approximation diagrams for the scattering of two nuclei.

Fig. 2. The simplest corrections to the optical approximation which correspond (together with the diagrams of Fig. 1) to the rigid target approximation for the scattering of two nuclei.

Fig. 3. The distribution on the stripping electrical charge of the projectile in $C-Ta$ interactions at 4 GeV per nucleon and its description by rigid target approximation [12].

Fig. 4. Predictions for the associated multiplicity distribution for $W^\pm$ and Z^0 events (round black points) together with the experimental data ($W^\pm$ cross points and Z^0 white stars) and the minimum bias distribution (squares).

Fig. 5. The x_F-spectra of secondary π^+ (a), π^- (b), K^+ (c) and K^- (d), produced in pp interactions at 100 and 175 GeV/c [42] and 400 GeV/c [43]. The curves are the Quark-Gluon String Model predictions.

Fig. 6. The rapidity spectra of secondary π^+, π^- (a), K^+, K^- (b) and p, $\bar{p}$ (c) produced in $Pb+Pb$ interactions at 158 GeV/c per nucleon [45]. The curves are the Quark-Gluon String Model predictions.

References

[1] Yu.M.Shabelski. Yad.Fiz. 51 (1990) 1396.
D.Krpic and Yu.M.Shabelski. Yad.Fiz. 52 (1990) 766; Z.Phys. C48 (1990) 483.

[2] H.L.Bradt and B.Peters. Phys.Rev. 77 (1950) 54.

[3] Yu.M.Shabelski. Acta Phys. Polonica B10 (1979) 1049.

[4] V.M.Braun and Yu.M.Shabelski. Int.J. of Mod.Phys. A3 (1988) 2417.

[5] V.N.Gribov. ZhETP 56 (1968) 892; 57 (1969) 1306.

[6] O.V.Kancheli and S.G.Matinyan. Yad.Fiz. 11 (1970) 1305.

[7] W.Czyz and L.G.Maximon. Ann.Phys. 52 (1969) 59.

[8] V.Franco and G.K.Varma. Phys.Rev. C18 (1978) 349.

[9] Yu.M.Shabelski. Yad.Fiz. 47 (1988) 1612.

[10] G.D.Alkhazov et al. Nucl.Phys. A220 (1977) 365.

[11] R.D.Viollier and E.Turtschi. Ann.Phys. 124 (1980) 290.

[12] A.P.Gasparyan, A.P.Cheplakov and Yu.M.Shabelski. Yad.Fiz. 34 (1981) 1328.

[13] C.Pajares and A.V.Ramallo. Phys.Rev. C16 (1985) 2800.

[14] I.V.Andreev and A.V.Chernov. Yad.Fiz. 28 (1978) 477.

[15] I.V.Andreev and L.A.Khein. Yad.Fiz. 28 (1978) 1499.

[16] A.S.Pak et al. Yad.Fiz. 30 (1979) 102, 343.

[17] M.A.Braun. Yad.Fiz. 45 (1987) 1525.

[18] K.G.Boreskov and A.B.Kaidalov. Yad.Fiz. 48 (1988) 575.

[19] A.M.Zadorozhnyj, V.V.Uzhinsky and S.Yu.Shmakov. Yad.Fiz. 39 (1984) 1165.

[20] V.Franco and R.J.Glauber. Phys.Rev. 142 (1966) 1195.

[21] Yu.M.Shabelski and D.Treleani. Eur.Phys.J. A2 (1998) 275.

[22] V.A.Abramovsy, V.N.Gribov and O.V.Kancheli. Yad.Fiz. 18 (1973) 595.

[23] Yu.M.Shabelski. Nucl.Phys. B132 (1978) 491.

[24] A.Bialas, M.Bleszynski and W.Czyz. Nucl.Phys. B111 (1976) 461.

[25] C.Pajares and Yu.M.Shabelski. Phys.Atom.Nucl. 63 (2000) 908; hep-ph/9811214.

[26] J.Dias de Deus and R.Ugoccioni. Phys.Lett. B494 (2000) 53.

[27] A.Capella, A.Kaidalov and J. Tran Thanh Van. Heavy Ion Phys. 9 (1999) 169.

[28] Yu.M.Shabelski. Z.Phys. C57 (1993) 409.

[29] M.G.Ryskin and Yu.M.Shabelski. Z.Phys. C48 (1990) 463.

[30] G.J.Alner et al. Z.Phys. C33 (1986) 1.

[31] S.Backovich, D.Krpic and Yu.M.Shabelski. Z.Phys. C53 (1992) 613.

[32] Yu.M.Shabelski. Sov.J.Nucl.Phys. 50 (1989) 149.

[33] J.Dias de Deus, C.Pajares and C.A.Salgado. Phys.Lett. B407 (1997) 335.

[34] J.Dias de Deus, C.Pajares and C.A.Salgado. Phys.Lett. B408 (1997) 417.

[35] J.Dias de Deus, C.Pajares and C.A.Salgado. Phys.Lett. B409 (1997) 474.

[36] J.Dias de Deus and C.Pajares. Phys.Lett. B442 (1998) 395.

[37] A.B.Kaidalov and K.A.Ter-Martirosyan. Yad.Fiz. 39 (1984) 1545; 40 (1984) 211.

[38] A.B.Kaidalov and O.I.Piskunova. Yad.Fiz. 43 (1986) 1545.

[39] Yu.M.Shabelski. Yad.Fiz. 44 (1986) 186.

[40] A.B.Kaidalov, K.A.Ter-Martirosyan and Yu.M.Shabelski. Yad.Fiz. 43 (1986) 1282.

[41] Yu.M.Shabelski. Z.Phys. C38 (1988) 569.

[42] A.E.Brenner et al. Phys.Rev. D26 (1982) 1497.

[43] M.Aguilar-Benites et al., LEBC-EHS Coll. Z.Phys. C50 (1991) 405.

[44] G.H.Arakelyan et al. hep-ph/0103337.

[45] F.Sikler et al., NA49 Coll. Nucl.Phys. A661 (1999) 45c.

[46] A.Capella and C.A.Salgado. Phys.Rev. C60 (1999) 054906.

[47] A.Capella and A.Kaidalov. Heavy Ion Physics 9 (1999) 169.
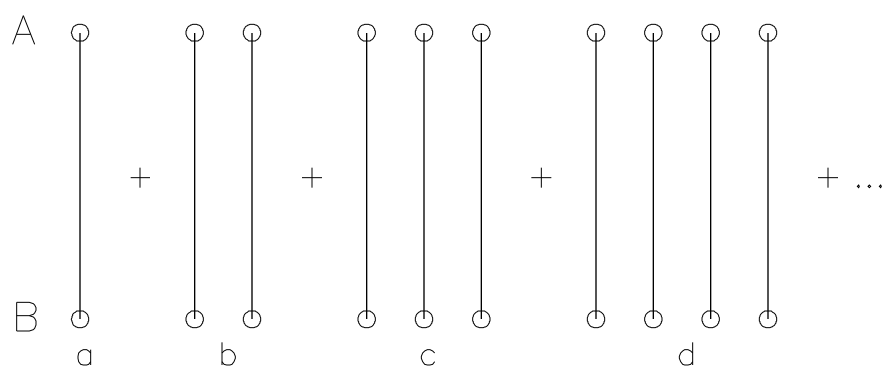
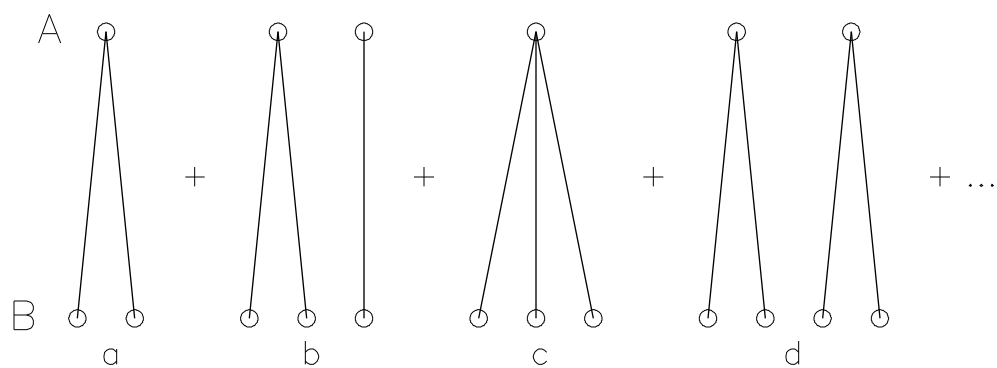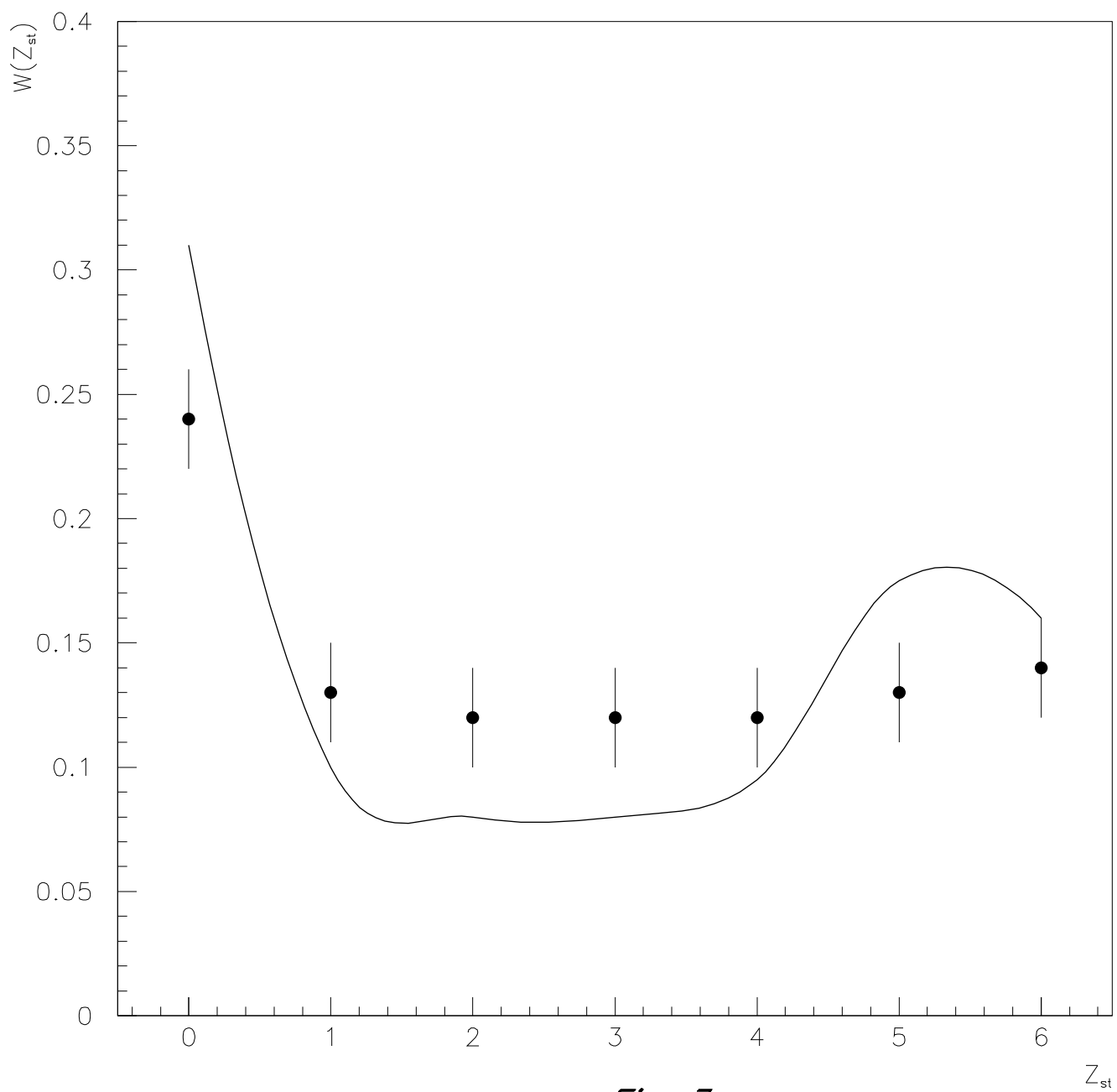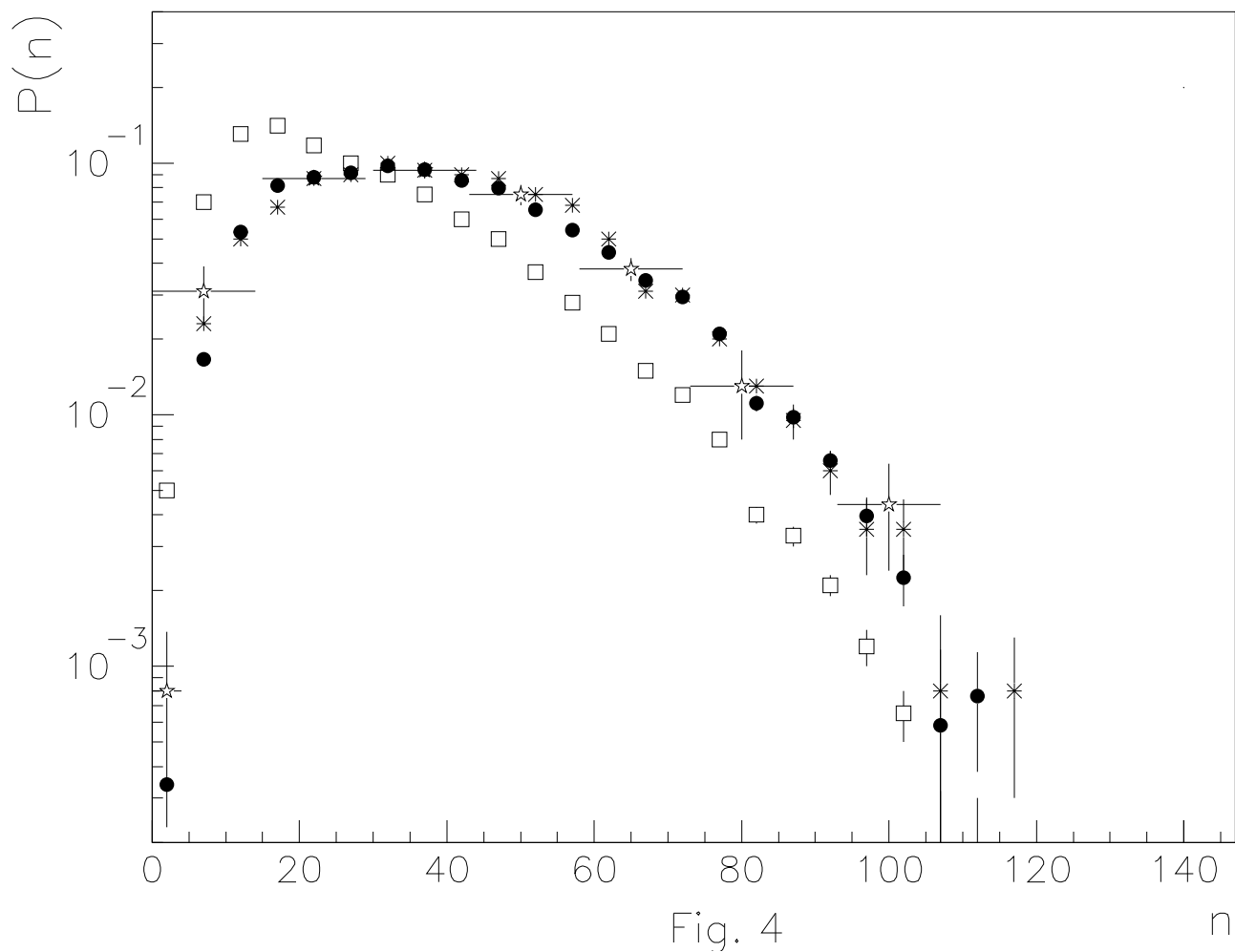[48] N.Armesto, C.Pajares and D.Sousa. hep-ph/0104269.

A   o   o o   o o o   o o o o

$$+ \quad\quad + \quad\quad\quad\quad + \quad\quad\quad\quad + \; ...$$

B   o   o o   o o o   o o o o
    a   b   c   d

Fig. 1

Fig. 2

Fig. 3

Fig. 4

Fig. 6b

PbPb → p̄,p X , A∗158 GeV/c

p ▲ and ————

p̄ ▼ and ------

Fig. 6c

Fig. 6a

Fig. 5d

Plot axes and labels:

- Y-axis: $x_F \, d\sigma/d \, x_F$, mb
- X-axis: x_F
- Annotation: $pp \rightarrow K^- X$
- $400 \, GeV/c$

Fig. 5c

$x_F \, d\sigma/dx_F$, mb

$pp \rightarrow \pi^- X$

400 GeV/c

Fig. 5b

x_F

Fig. 5a